Mitigation of Slamming of Catamarans in Waves

Ahmed Swidan[1, 2*], Dane Christophersen[3], and Tristan Bauer[4]

[1]UNSW Canberra at ADFA, Australia. A.Swidan@unsw.edu.au
[2]Arab Academy for Science, Technology and Maritime Transport, Egypt.
[3]Royal New Zealand Navy, New Zealand. danechristophersen@gmail.com
[4]Austal, Australia. tristan.bauer@utas.edu.au

High-speed catamarans have, over the past three decades, extended their service areas from protected waters to the open ocean where impacts with waves can result in structural damage. The work detailed in this paper investigates the wetdeck slamming loads experienced by an amended NPL model that is equipped with a centrebow between the two demihulls while encountering regular waves. The investigation centred on the influence of early flow separation through utilising three interchangeable centrebow configurations and assessing the slam force magnitudes. The systematic and random uncertainties associated with the seakeeping test results are quantified in detail. This experimental investigation therefore provides a new dataset for the slam forces on an arched wetdeck structure of catamaran vessels in head seas. It was found that the early water separation when employing two wedge sections would reduce the slam forces by approximately 44% when compared with the parent centrebow configuration. The proposed new passive technique presents a step forward towards lighter and faster catamarans.

INTRODUCTION

A catamaran experiences wetdeck slamming when operating in large waves as the wetdeck, the exposed deck area between the two demi hulls of the catamaran, impacts the water surface with a high relative vertical velocity. Wetdeck slamming is a significant design issue for catamarans since it can decrease catamarans' transport efficiency and can cause major structural damage and avoiding its occurrence is one of the main reasons a vessel's master will reduce speed or change course in heavy weather, adversely affecting the vessel's operation and schedule.

During operation within the normal limits of a typical catamaran only the demihulls interact with the water. Operating in sufficiently large sea states, pitch and heave motions may cause the lower most exposed surface of the cross-deck structure connecting the hulls, known as the wetdeck, to impact the water surface. With repeated loading and unloading, fatigue failure becomes increasingly likely, and previous catastrophic failures of catamarans have occurred, despite being designed to classification society rules (Swidan, 2016).

Figure 1: Saint John Paul II, wave piercing catamaran, length overall = 110m (Incat, 2019).

A centrebow is intended to enhance catamaran performance in rough seas by damping the heave and pitch motions, as commonly included in INCAT's Wave Piercing Catamaran (WPC) designs, as shown in Figure 1. In comparison to conventional catamaran demihulls the high slenderness ratio of WPCs provides little reserve buoyancy to dampen pitch and heave motions, increasing the likelihood of the wetdeck contacting the water surface and a corresponding increase in the number of slamming occurrences. A centrebow can be described as a partial arched bow form which is truncated at typically 0.2-0.33 LOA and then a flat wetdeck continues aft towards the stern.

The central keel of the centrebow is located slightly above the calm water surface at full load displacement and static trim to avoid unnecessary resistance while operating in slight seas, as shown in Figure 1. Under rough sea conditions which would induce sufficient vessel motions, the centrebow enters the water at relatively high vertical velocities, consequently producing severe slam loads. The addition of a centrebow is beneficial to the catamaran design, although it increases the overall complexity and light ship weight of the vessel. An investigation into the magnitude of the slamming forces and induced loads on a WPC model demonstrated that slam induced bending moments were found to reach 11% of the product of hull weight x length, and the slam loads were found to reach as high magnitude as 132% of the hull weight (Davis, et al., 2017). A range of centrebow geometries, e.g. relatively longer and shorter centrebows, have been tested to explore whether there are significant improvements available to reduce the severity of the slamming loads. It was found that the larger centrebow volume induces larger slam loads due to an increase in the volume of trapped water (Shahraki, 2013). Relatively shorter centrebows were determined to displace water forward of the demihull bows, thereby minimising the developed slamming loads (Shabani, 2017).

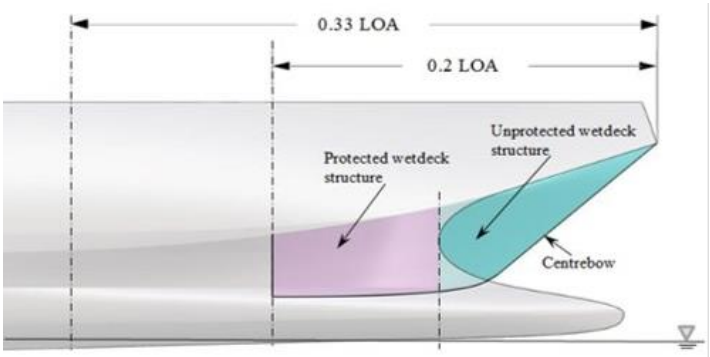

Figure 2: Showing the main area of interest in the design of high-speed catamarans, which is the impact loading in the vicinity of the centrebow (Swidan, 2017).

Controlling the vessel motions have also been explored, where an active T-foil was included at the bow in conjunction with stern tabs. The study showed a potential in reducing the motions when the system was passive, although not as effective (AlaviMehr, 2016). Modifications to the geometry which intentionally influences the flow can potentially offer reduction in the slamming loads (Swidan, 2016).

It is desirable to explore potential methods to minimise wetdeck slamming while maintaining the benefits that the centrebow offers. The purpose of this research was to investigate the effect of a passive device on reducing the total slamming load experienced by a generic catamaran hull model fitted with three centrebow configurations.

MODEL AND EXPERIMENTAL SETUP

The Test System

The model tests were performed in the towing tank facility of the Australian Maritime College (AMC), see Figure 3. The AMC's towing tank is 100 m long by 3.55 m wide. Experiments are generally carried out at a water depth of 1.5 m depending on the size and type of model being tested. In this study, a water depth of 1.4 m was necessary to avoid model to carriage possible collisions due to the expected magnitude of model motions. Two disadvantages were recognized utilizing this set-up, 1. the wave-damping mechanism along the side of the tank was ineffective, and 2) the wave maker is calibrated for a water depth of 1.5 m, as such there were slight differences between the target wave heights and the achieved ones during the experimental tests. The hydraulically operated single flap paddle type wave generator produces waves with wavelengths of 0.4-6.5 m and 0.4 m high. A PC based DAQ and processing system is provided to which a variety of analogue and digital instruments can be connected.

The Test Model

The test model was constructed using the National Physics Laboratory (NPL) demihulls and fitted with a generic centrebow, that looks like those used by INCAT, see Figure 4. Figure 4 shows the body plan of the developed catamaran model with the parent centrebow. The model's main particulars are presented in Table 2.

Figure 3: Showing the test model attached to the carriage of the towing tank facility at the Australian Maritime College, encountering a wave height of 72.7 mm at a speed of 1.53 m/s.

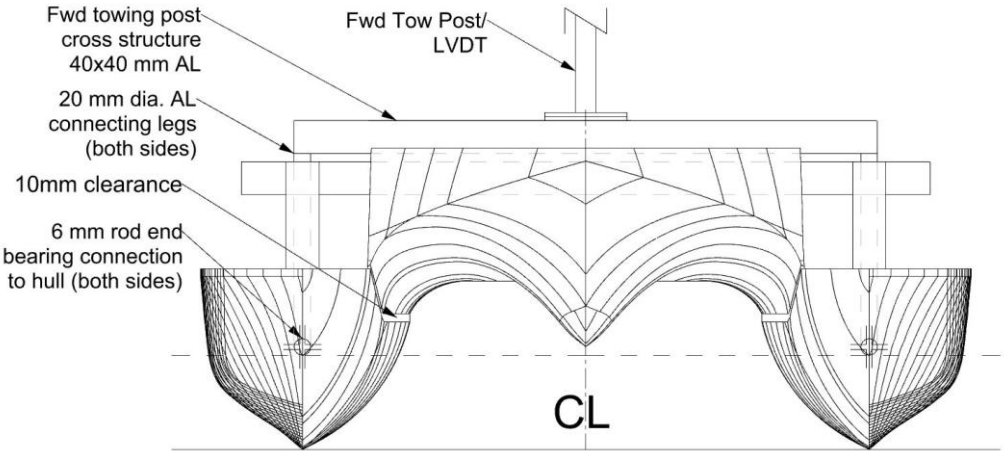

Figure 4: Body plan of the NPL's demihulls fitted with a generic centrebow and the forward towing configuration.

Table 1: Main particulars of the test model

Length Overall	2661 mm
Length Waterline	2502 mm
Displacement	52.16 kg
Draft	115 mm
Beam at waterline	918 mm
Beam Centres	690 mm
LCG (model) from transom	1162 mm
Pitch radius of gyration (about LCG)	893

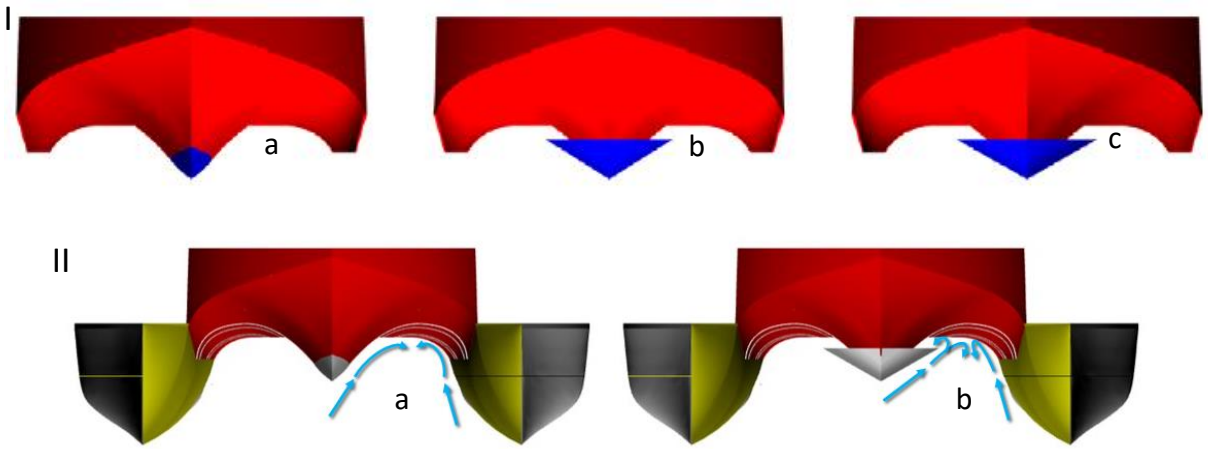

Figure 5: I-(a) Showing the parent centrebow; (b) 35 mm wedge fitted to parent centrebow; (c) 45 mm wedge. (a), (b) and (c) are viewed from forward and omit the demihulls. Figure 3 II-a showing the semi-entrapped flow behaviour between the parent centrebow and the demihull, (b) illustrates an early flow separation around the tip of the 35 mm wedge.

To study the influence of an early flow separation on the wetdeck slam force magnitudes, two interchangeable wedge sections were designed, 3D printed and fitted on the parent centrebow, see Figure 5-I and 5-II. These three model configurations, namely: parent, 35 mm wedge and 45 mm wedge, are shown in Figures 5-I and 6. Figure 6-a shows the width of the horizontal face of the wedges were set to 35 mm and 45 mm, which occupied approximately 20% and 25% of the 180 mm tunnel width at the centrebow truncation, respectively.

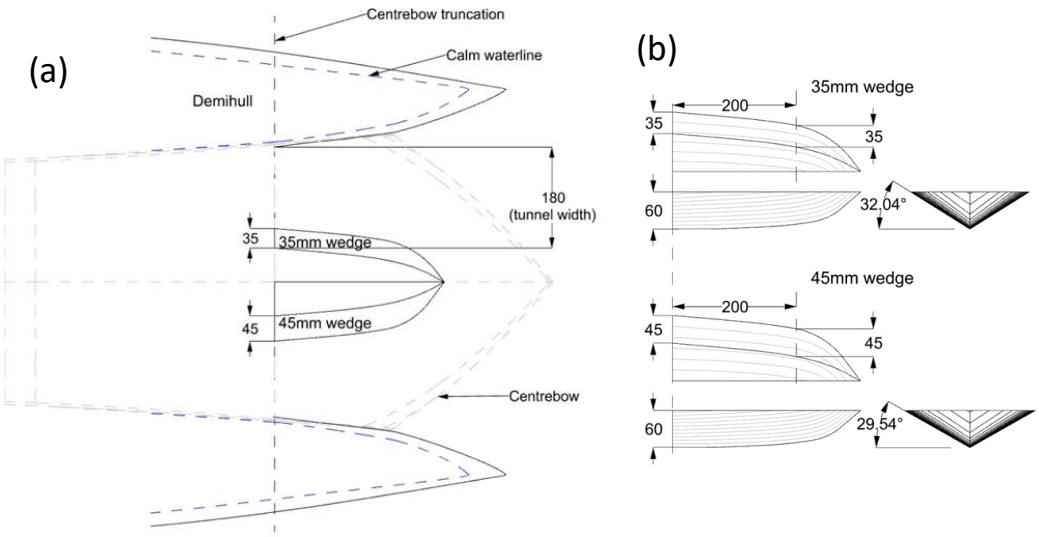

Figure 6: Showing (a) the horizontal faces that occupy 20% and 25% of the tunnel width on a plane 70 mm above the waterline for the 35 mm and 45mm wedge respectively, and (b) the lines and principal geometry of the 35mm and 45mm wedge sections.

Figure 6-b shows the overall height of the wedge section (applicable to both wedges) at the aft extent was 60 mm which reduced toward the bow to follow the keel line of the parent centrebow. The wedges are henceforth referred to as 35 mm and 45 mm which relates to the width of the horizontal surfaces. The increase in volume over the parent centrebow due to the wedges was 0.4946x10-3 m^3 and 0.6371x10-3 m^3 for the 35 mm and 45mm wedge respectively.

Instrumentation

To characterise the model's response during impact, the key parameters measured in these model tests were; the vertical force, wave profile, heave, pitch and the carriage speed. A summary of the instruments and signal conditioning hardware is given in Table 2.

Three load cells were considered to be the minimum number sufficient to avoid moments during the impact phase based on recent drop-test experiments, such as those of Swidan et al. (2016). All the total impact force measurements presented in this paper are the sum of the three load cell outputs, as shown in Figure. 7. The model was attached to the carriage by two tow posts, allowed to move freely in the vertical direction within linear slides, to which DC-EC series LVDT sensors were attached to capture pitch and heave data.

Table 2: Details of Gauges

Gauge	No. of Channels	Manufacturer	Model	Maximum Range
Carriage speed	0	SICK	DME5000	150 m
Load cell	3	Applied Measurement	S1W	350 N
LVDT	3	Hampton	DC-EC-5000	
Static wave probe	2	Static wave probe		0.5 m
Moving wave probe	2	General Acoustics	USS 20130	0.5 m

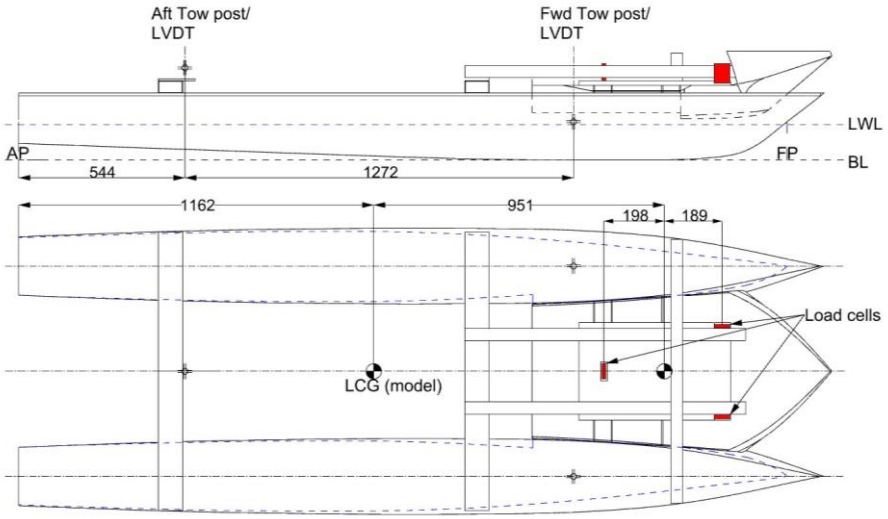

Figure 7: Plan and profile views of the model setup showing locations of load cells and tow posts

Wave heights were recorded primarily by a static wave probe located 9 m forward of the wave-maker. Supplementary to this were two moving wave sensors to capture the instantaneous wave profile the model was encountering. These were attached to the carriage with one abreast the LCG of the centrebow and the other abreast the LCG of the model, set as far outboard as possible to avoid any bow wave or wake while avoiding wall effects of the towing tank. This was achieved by conducting several calm water runs with a rigidly fixed reference set very near the water surface and observing any disturbance to the water surface. Minor seiching was observed with a long standing wave with a period of approximately 45 s which affected this process, therefore the best compromise was used. It was assumed the seiching was a consequence of the reduced water depth used and would not influence the final results due to the very long wavelength and elimination through post processing methods. Settling time of the tank between runs was maintained at approximately 45 min between runs due to the wave dampening mechanisms on the side of the towing tank being unavailable at a water depth of 1.4 m.

The load cells were calibrated off the model by suspending each from a rigid point and applying known masses. This was checked both when applying and removing the masses to ensure the output was a linear relationship and was repeatable. Once the load cells were applied to the model, the loads were zeroed by the associated wheatstone bridges and a check was performed to ensure the total load output from all three load cells were producing an accurate load output. A known weight was placed in three arbitrary positions along the centrebow and the 'record zeros' function in the DAQ system captured the load values from each load cell. This also provided confidence that there was no noticeable binding in the model setup and that the load cells would carry the entirety of the applied load.

A video camera recording at 1920 x 1090 resolution at 25 frames per second was set up immediately forward of the vessel as close to the water surface as possible to view the flow within the centrebow tunnels. The signals from all the instruments were acquired using a modular National InstrumentsTM compact data acquisition system (cDAQ 9174) with National Instruments LabVIEW software used to record the signals. A sampling rate of 10 kHz was used. The measured data was automatically converted into its corresponding unit of measured data using the calibration factors that were input into the DAQ software prior to the tests.

Test Conditions

Tests in irregular waves and oblique seas are recommended for testing catamaran operational limits and for determining extreme phenomena, however this presents an increase in the number of variables and associated complexity in analysis (ITTC, 1999). This investigation was limited to regular head seas to provide high-quality data that could be used as benchmark for validating numerical methods by designers and researchers. The three centrebow configurations were all subject to the same test conditions. Overall, there were 18 conditions in total, with 3 test runs each to ensure repeatability of the recorded data. Prior to the testing starting, 20 runs were performed to assess the model and instrumentation quality. The two model speeds of 1.53 m/s and 2.89 m/s, and initial wave frequency of 0.8Hz were common with previous studies, e.g. by AlaviMehr (2016).

The equivalent Froude number of the speeds of 1.53 m/s and 2.89 m/s are of 0.31 and 0.58 respectively, which would represent 20 and 38 knots respectively for a full-scale vessel assuming an approximate scaling factor of 45. Each tested wave height of 75, 90 and 105 mm was non-dimensionalised against the wavelength to give corresponding wave frequencies of 0.876, 0.8 and 0.741Hz, respectively. To present the measured data, the frequencies are shown in non-dimensional circular encounter frequency, w_e^*, which factors in the models heading and speed with respect to the waves. The formula is presented in equation (1).

$$w_e^* = 2\pi f_e \sqrt{\frac{Lwl}{g}} \qquad (1)$$

Table 3: Summary of Test Conditions

Configuration	Speed [m/s]	Wave height [mm]	Corresponding wave frequency [Hz]
Parent model hull	1.53	75, 90 and 105	0.876, 0.8 and 0.741 respectively
	2.89	75, 90 and 105	0.876, 0.8 and 0.741 respectively
With 35mm Wedge	1.53	75, 90 and 105	0.876, 0.8 and 0.741 respectively
	2.89	75, 90 and 105	0.876, 0.8 and 0.741 respectively
With 45mm Wedge	1.53	75, 90 and 105	0.876, 0.8 and 0.741 respectively
	2.89	75, 90 and 105	0.876, 0.8 and 0.741 respectively

The average water temperature was 18°C, the average air temperature was 20°C and the density of the water was 998.85kg/m^3 for the duration of the testing (ITTC, 2011). The test conditions are summarised in Table 3.

UNCERTAINTY ANALYSIS

To ensure the high quality of the measured data, systematic and random uncertainties were determined. Systematic uncertainties stem from the instrument themselves, and the accuracy of the reading is usually published by the manufacturer. Random uncertainties are caused by factors which are uncontrolled, e.g. environmental.

Systematic Uncertainties

The uncertainties based on the instrumentation used were sourced from the technical data provided by the manufacturers.

Table 4: Summary of the systematic uncertainty of the instruments

	Carriage position/speed	Load cell	LVDT	Moving wave sensor
Uncertainty source	Waldkirch DME5000-212	VA DC- EC-5000(MC)	XSENS MTI-10 series	General Acoustics 20130
Linearity error (%)	0.3	0.03	0.25	0.18

Table 4 summarises the systematic uncertainties of each instrument used during the experiment. The linearity error is the residual difference between the sensor output curve and line of best fit.

Filtering of measured slam forces has been avoided to obtain the peak of the transient slam load magnitudes that occurs within a very short duration of time. Butterworth low pass filter was utilized to attain velocities from positional data by taking the gradient between incremental data, filtering was necessary to eliminate noise in the source data.

Random Uncertainties

Each condition, see Table 3, was repeated for a minimum of three runs to confirm that the recorded data was repeatable. Additionally, it helped to provide confidence in the instrumentation being used including the recording DAQ system.

Figure 8 shows a good agreement between the repeated three tests of all measured data using two LVDTs, static wave sensor, carriage speed sensor, and three identical load cells. Figure 8 illustrates three runs at 1.53 m/s set carriage speed and 90 mm set wave heights at a set wave frequency of 0.8 Hz.

The root mean square error (RMSE) for the peaks of the forward LVDT was 1.43 mm and the aft LVDT RMSE was 1.45 mm over 10 cycles, as shown in Table 5. The steps in the wave data is due to the 50 Hz output of the wave sensor being sampled at 10 kHz as previously described.

The carriage speed showed good repeatability across all runs. The static wave probe showed some uncertainty in the wave height produced by the wave generator, as shown in Table 5, with the greatest error found for the wave height of 90 mm at ±6.27%. The total wave height did not achieve the desired magnitude, and this was likely caused by the lowering of the towing tank depth to 1.4m. The amplitude heave motions were compared to assess the repeatability of the forward and aft LVDTs. The results showed the peaks to be uncertain within 5%. Figure 8 presents the achieved wave heights (H_w) of 84 and 101 mm with a maximum deviation of 6.25% with the target wave heights of 90 and 105 mm, respectively.

The typical cyclical loading on each of the load cells for three repeatability runs using the parent configuration in 105 mm waves and 1.53 m/s carriage speed, is presented in Fig. 8.

Table 5: Summary of recorded wave heights and their respective RMSE and percentage error

Average Wave Height [mm]	RMSE ± [mm]	Error ± [%]
72.74	0.6	1.65
83.71	2.6	6.27
101.19	0.36	0.72

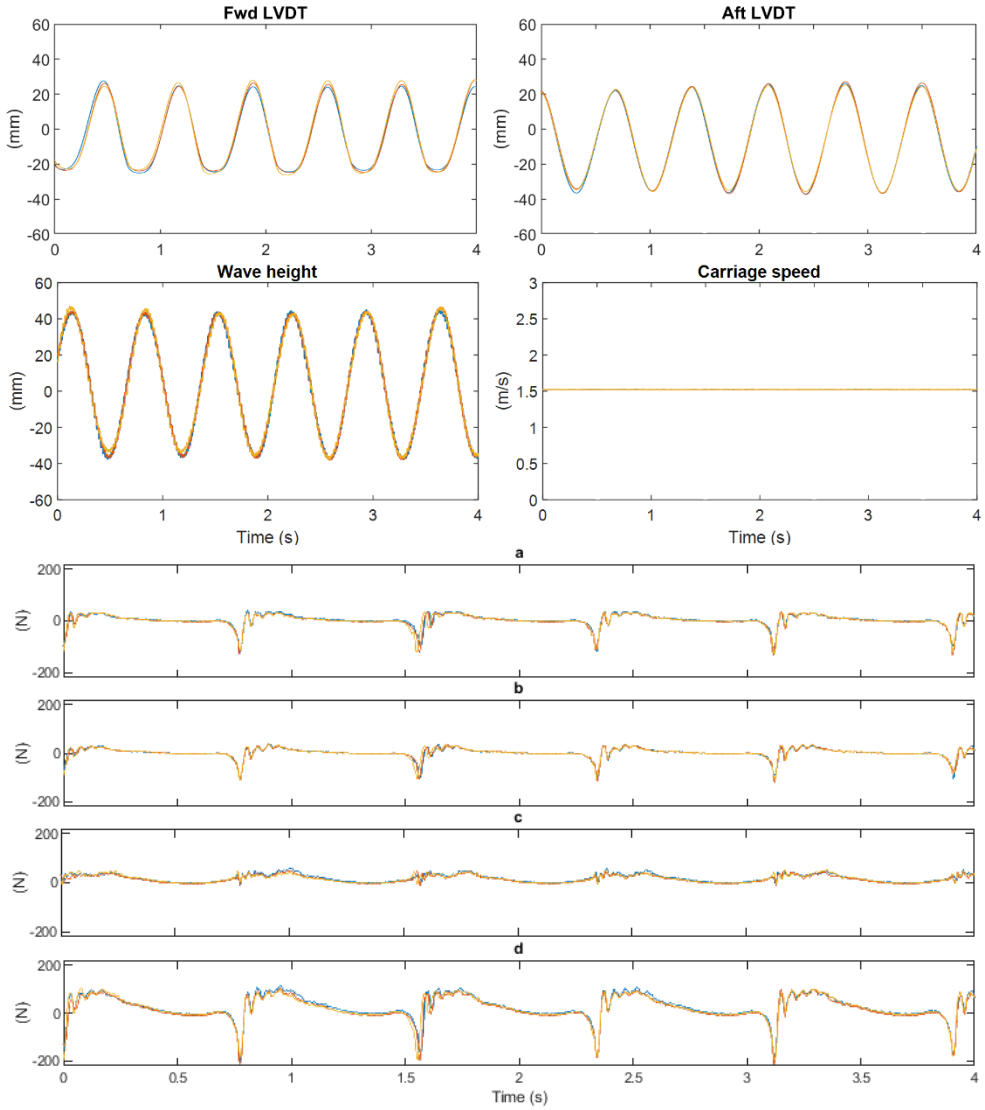

Figure 8: Showing 3 run results of condition 1. The results include the aft and Fwd LVDTs, static wave height sensor, carriage speed, and the measured forces of (a) the port side load cell, (b) starboard load cell, (c) Aft load cell, and (d) The total load, e.g. instantaneous summation of the three load cell measurements.

The asymmetrical loading was approximately 9.95% greater on the starboard load cell. This was likely due to the asymmetrical mass of the centrebow due to the plugs where pressure sensors have previously been fitted. These results ensured high-quality experimental data that provides a benchmark for researchers and industry performing numerical and computational simulations.

RESULTS AND DISCUSSION

The presence of wetdeck slam events, where water impacted the archways, was limited to 9 conditions, are summarised in Table 6 with the achieved wave height. The wave length, λ, was calculated from $\lambda = g/\omega^2 2\pi$, with an initial wave frequency, f, selected as 0.8Hz based on previous experiments of a similarly sized model (AlaviMehr, 2016). The non-dimensional wave height, h_w, was constant for all conditions and calculated from $h_w = kHw/2$, where k was the wave number calculated by $k = 2\pi/\lambda$.

Non dimensional wave circular encounter frequency, ω_e, was calculated by $\omega_e = \omega + \omega^2 V_m/g$, where V_m is the model velocity. The wavelength, λ with an initial wave frequency, f, is selected as 0.8 Hz based on recent tests of a similarly sized model by AlaviMehr (2016). Table 6 presents, the non-dimensional wave height, h_w, k that is the wave number calculated, w_e^*, which is the non-dimensional wave circular encounter frequency and V_m equal to the model velocity.

Figure 9 illustrates a corresponding load cycle for both the parent centrebow and the 45 mm wedge configuration in condition '1'. The major characteristics of the trend for the parent centrebow are labelled in Figure 9-a. Figure 9-b shows the introduction of a small peak in the total load prior to the maximum slam load, when the wedge impacts with the water surface. This minor depression was likely to be significantly reducing the subsequent major slam load. An overlay of the two data sets is shown in Figure 9-c to demonstrate there is a clear difference in the magnitude of the maximum slam load and subsequent vibration, and similar load throughout the remainder of the cycle.

Figure 10 illustrates that the wedge is forcing water transversely outwards during water entry, disrupting the flow of the jet rising up the sides of the demihulls, and the highly turbulent flow within the tunnels is also a possible contributing factor for reducing slam load magnitudes due to the higher air content. It was probable that there was a region of trapped air above the horizontal surfaces of the wedges during submersion, as there was visible flow separation occurring during the relative descent of the centrebow.

Figure 11 demonstrates consistency of the previously identified reduction in slam loads across the 10 s sample data for each configuration operating in a condition 'a'. Only the points of maximum load are shown to avoid confusion. Visual inspection of these plots indicates that the parent centrebow repeatedly experiences the highest slamming loads, while the 45mm wedge offers the greatest reduction. Table 7 presents the mean load and percent reduction for each configuration over the 10 s period.

Table 6: Summary of Test Conditions when Slam Occurred

	Condition	V_m [m/s]	H_W [mm]	h_w	f [Hz]	λ [m]	k	w_e [rad/S]	w_e^*
All hull forms	1	1.53	84	0.12	0.8	2.44	2.5	9.01	4.53
	2	1.53	101	0.11	0.74	2.85	2.2	8.04	4.06
	3	2.89	101	0.11	0.74	2.85	2.2	11.04	5.57

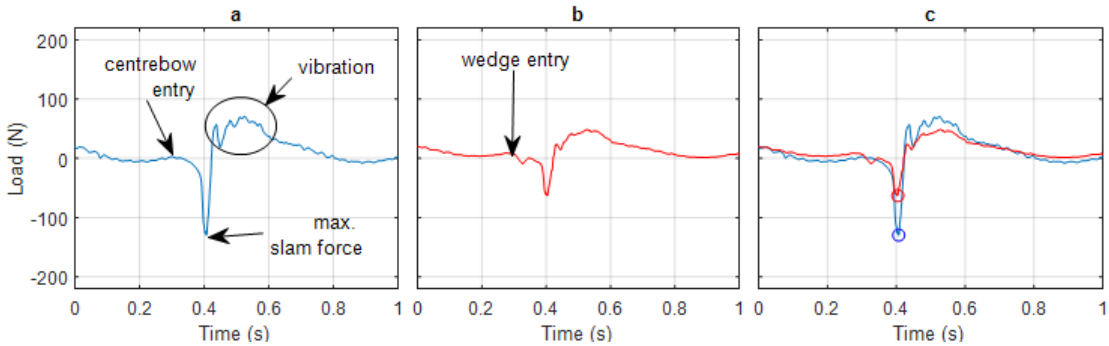

Figure 9: Showing a slam cycle load of (a) parent and (b) 45mm wedge configurations in condition '1', and (c) compares between the two configurations.

Table 7: Mean peak load amplitude and percentage comparison per each configuration

		Mean peak force magnitude [N]			Mean peak force [%]		
	Condition	(1)	(2)	(3)	(1)	(2)	(3)
Configuration	Parent	-125	-186	-129	100	100	100
	35mm wedge	-87	-135	-105	69.6	72.6	81.4
	45mm wedge	-55	-112	-90	44	60.2	69.8

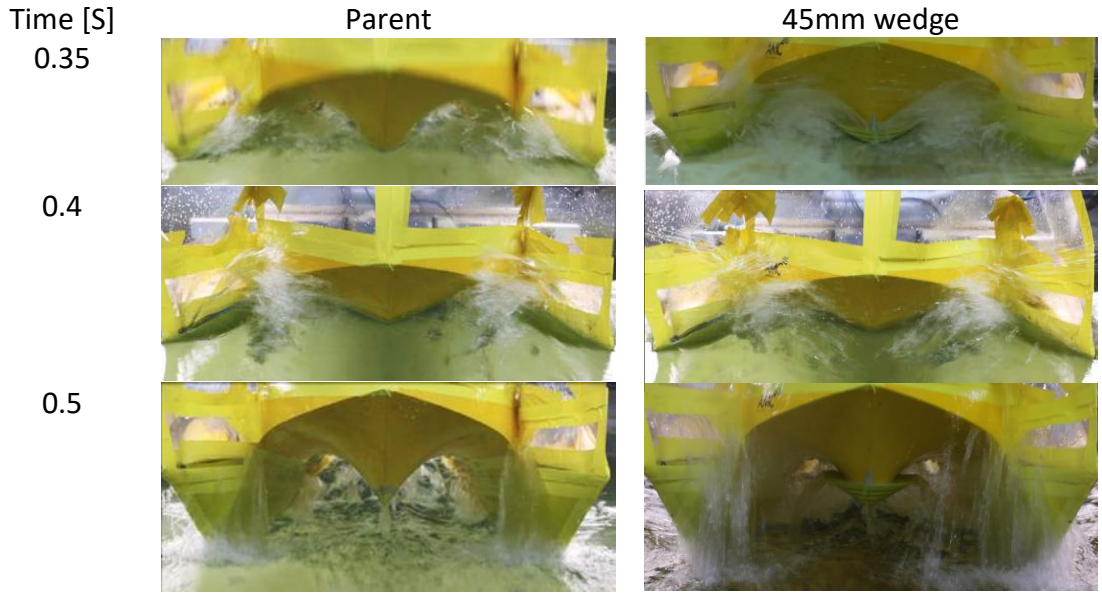

Figure 10: Photos taken of the parent and 45mm wedge configurations during a slam cycle.

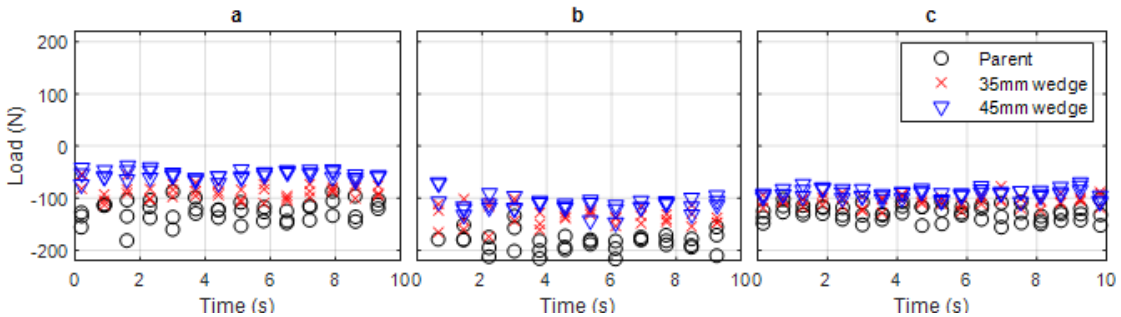

Figure 11: Showing all measured slam peak force magnitudes of conditions 1, 2 and 3.

CONCLUSIONS

This paper reported on a series of seakeeping tests to investigate the influence of early flow separation on the wetdeck slam force magnitudes by utilizing a generic catamaran hull model that is fitted with three centrebow configurations during wave impacts. In contrast to previous seakeeping tests these experiments focuses on reducing wetdeck slamming loads by allowing the flow to separate prior to slam event rather than modifying using larger or shorter centrebow configurations.

Since full details of the generic hull form are presented the results provide a comprehensive set of benchmarking data for use in the validation of numerical techniques to predict slam impact magnitudes of catamarans encountering regular waves.

The systematic and random uncertainties associated with the towing tank test results were quantified in detail and demonstrated the excellent repeatability of the tests; for example, the uncertainty of the measured peak slam loads was found to be less than 10%.

The developed wedge centrebow geometry in this paper could be considered as a novel finding towards minimising wetdeck slam severity that would affect passenger comfort, hull structure, cargo lashing and machinery operations of catamarans. The largest reduction in total impact loads, observed when utilizing the 45 mm wedge to be approximately 44% of the parent centrebow in a test condition. Thus, the addition of a wedge to the centrebow of a WPC offers a potential passive device to minimise slam loads and there is benefit in pursuing the concept.

ACKNOWLEDGEMENTS

The Authors would like to acknowledge Dr Jason Lavroff for assistance in the experimental design as well as Mr Tim Lilienthal and Mr Kirk Myer for assistance in the model setup.

REFERENCES

AlaviMehr, J., 2016. The Influence of Ride Control Systems on the Motion and Load Response of a Hydroelastic Segmented Catamaran Model. PhD thesis, University of Tasmania, Hobart, Australia.

Davis, M. R., French, B. J. & Thomas, G. A., 2017. Wave slam on wave piercing catamarans in random head seas. Ocean Engineering, pp. 84-97.

Incat Tasmania (2019). 112m high-speed wave-piercing catamaran. Retrieved 18 Feb, 2019, from: http://www.incat.com.au.

ITTC. (2011). Fresh water and sea water properties. Hjortekaersvej 99: 26th ITTC Specialist Committee on Uncertainty Analysis.

Shabani, B. (2017). *The effects of tunnel height and centre bow length on motions and slam loads in large wave piercing catamarans.* PhD thesis, University of Tasmania, Hobart, Australia.

Shahraki, J. R. (2014). *The Influence of Hull Form on the Slamming Behaviour of Large.* PhD thesis, University of Tasmania, Launceston, Australia.

Swidan, A., Thomas, G., Ranmuthugala, D., Penesis, I., Amin, W., Allen, T. & Battley, M. Experimental drop test investigation into wetdeck slamming loads on a generic catamaran hullform. *Ocean Engineering*, vol. 117C, pp. 143-153. 2016.

Swidan, A. (2016). Wetdeck Slamming Loads– Experimental and Numerical Investigation. PhD thesis, University of Tasmania, Launceston, Australia.

Swidan, A., Thomas, G., Penesis, I., Ranmuthugala, D., Amin, W., Allen, T. & Battley, M. Wetdeck slamming loads on a developed catamaran hullform - Experimental investigation. *Ships and Offshore Structures*, vol. 1, pp.1-9. 2017.